Iranian Journal of Materials Forming 9 (4) (2022) 13-25

Online ISSN: 2383-0042

IJMF

Iranian Journal of Materials Forming

Journal Homepage: http://ijmf.shirazu.ac.ir

Research Article

Hot Ductility Behavior of the Electrolytic Tough Pitch Copper Having Different Initial Oxygen Content

H.R. Abedi[1*], A. Zarei-Hanzaki[2*], Z. Loghman Nia[3], M. Taherimandarjani[4] and A. Moshiri[2]

[1] School of Metallurgy & Materials Engineering, Iran University of Science and Technology (IUST), Tehran, Iran
[2] School of Metallurgy and Materials Engineering, College of Engineering, University of Tehran, Tehran, Iran
[3] Humboldt-Universität zu Berlin, Department of Chemistry, Brook-Taylor-Str. 2, 12489 Berlin, Germany
[4] Department of Mechanical and Product Design Engineering, School of Engineering, Faculty of Science, Engineering and Technology, Swinburne University of Technology, Hawthorn, VIC, 3122, Australia

ARTICLE INFO

Article history:

Received 24 June 2022
Reviewed 3 September 2022
Revised 26 September 2022
Accepted 26 September 2022

Keywords:

Tough pitch copper
Ductility trough
Oxygen content
Thermomechanical processing

Please cite this article as:

H.R. Abedi, A. Zarei-Hanzaki, Z. Loghman Nia, M. Taherimandarjani, A. Moshiri, Hot ductility behavior of the electrolytic tough pitch copper having different initial oxygen content, *Iranian Journal of Materials Forming*, 9(4) (2022) 13-25.

ABSTRACT

The possible ductility troughs of tough pitch copper containing various oxygen contents were identified to determine the safe and unsafe thermomechanical processing domains. Tensile and compression tests were conducted in temperature range of 300-800°C. The critical strain of single/multiple peaks dynamic recrystallization decreased by increasing oxygen content up to 220 ppm, and again increased with further increment up to 390 ppm. The non-uniform elongation region increased by increasing the temperature, and above 500°C, it was the dominant portion of the tensile curves. The long post-uniform elongation was attributed to the occurrence of dynamic recrystallization which increased the resistance of the material to localized necking. Two ductility troughs (unsafe thermomechanical processing regions) were recognized at temperatures of 400±50°C and 600±50°C. The ductility drop regions shifted to lower temperatures with an increase in the strain rate. The variation of the oxygen content, however, did not have significant effects on the position of ductility drops. The current work also explores the fracture surface characteristics of the tensile tested specimens.

1. Introduction

The hot ductility phenomenon and the occurrence of ductility minimum temperature (DMT) is one of the unexplained features of metal and alloy processing, which is observed as decreasing in elongation to fracture values in the range of 0.3-0.6 of melting point temperature [1, 2]. The ductility is mainly dependent upon the work hardening capacity of the material and the material's resistance against localized deformation. The former can be assessed through measurement of the strain hardening exponent (n-values), and the latter

* Corresponding authors
E-mail address: zareih@ut.ac.ir (A. Zarei-Hanzaki)
E-mail address: habedi@iust.ac.ir (H.R. Abedi)
https://doi.org/10.22099/IJMF.2022.44143.1232

through strain rate sensitivity (m-values) [3]. The higher strain rate sensitivity means the higher capability of strain distribution which delays the onset of localized necking under tensile stress and increases the portion of non-uniform elongation. Generally, the materials' formability is expected to improve by increasing the deformation temperature, owing to the activation of the secondary slip systems and the activation of new deformation mechanisms. However, it has been observed that the toughness and ductility may increase or decrease to an unacceptable level at various processing conditions. The ductility troughs at higher temperatures are attributed to various mechanisms such as strain concentration and flow localization in more ductile phases, grain boundary sliding followed by W-type/R-type cracking, incipient melting reactions and diffusional transformations [2, 3]. The ductility decrement at a higher temperature has been previously reported in many metals and alloys such as steels [3-5], copper alloys [6, 7], titanium alloys [8], magnesium and aluminum alloys [9-11].

Due to its superior ductility, thermal/electrical conductivity, and corrosion resistance, pure copper has found a widespread application in the plastic forming of near-net-shape products. In this respect, the flow stress behavior of pure copper has drawn the attention of numerous researchers, the majority of which have focused on micro-deformation behavior [12-15] and severe plastic deformation methods [16, 17]. The effects of stacking fault energy [18, 19], and grain size [20] in correlation with the strain hardening behavior [21], and even mechanical twinning [22] have also been discussed in detail. The high temperature forming has been widely employed to obtain copper parts with complex shapes. Therefore, to optimize the fabrication process, investigating the high temperature deformation behavior of pure copper is highly necessary. In this respect, many researchers have pointed out the occurrence of dynamic recovery and dynamic recrystallization in a wide range of temperature and strain rates, the constitutive equations predicting flow stress have been developed and the processing maps have been constructed [23-25]. The results show that the corresponding stress-strain curves are characterized by multiple peaks or a single peak flow and reaching a steady state regime at high strains. In this regard, Belyakov et al. [26] have also investigated the deformation behavior of pure copper in warm temperature deformation regime (0.3-0.5 T_m) where, by increasing the temperature, the pancake-deformed microstructures have been changed into the refined microstructure accompanied by the transition from athermal to thermal flow behavior.

The main points which have been mainly overlooked in previous literatures are: (i) characterization of the possible ductility troughs during high temperature deformation of pure copper and (ii) the effect of oxygen content on the hot deformation characteristics of the material. The presence of oxygen not only influences the thermal/electrical conductivity but is also expected to significantly affect the strain accommodation capability of the copper and its susceptibility to micro-cracking. Towards this end, in the current study, the warm to hot ductility behavior of tough pitch copper containing various oxygen contents has been precisely studied by conducting hot tensile testing methods that would determine the safe and unsafe thermomechanical processing domains as well as characterize possible ductility drops and related deformation mechanisms. The hot compression tests have also been scheduled in the same deformation condition to properly assess the occurrence of dynamic restoration processes.

2. Experimental

Polycrystalline copper rods with a diameter of 8 mm were prepared through cold rolling and annealing of the electrolytic tough pitch (ETP) copper with a purity of 99.99%. These were received from the Sarcheshmeh Copper Industries, the oxygen content of which lay in a range of 100-700 ppm. A highly pure copper material, such as oxygen-free copper (OFC) or tough pitch copper (TPC), is suitable for high-end acoustic equipment and signal cables. The oxygen content may significantly affect both performance and quality, so the accurate quantification of the oxygen concentration is essential. In the present work, the determination of oxygen has

been conducted through inert gas fusion according to the ASTM E2575 standard. This test method is capable of covering the oxygen content in copper and copper alloys in a range of 0.00035% to 0.090%. Considering the copper-oxygen equilibrium phase diagram [27], the maximum solid solubility of the oxygen is about 50 ppm at 900°C, and it is in the form of Cu_2O particles at higher concentrations. In this respect, the Cu_2O volume fraction of treated structures was calculated according to the Cu_2O equilibrium phase diagram and represented in Fig. 1, which would be raised with oxygen content increment.

In order to assess the high-temperature formability of O-contained (160, 220, 390, and 660 ppm) copper alloys, isothermal hot tensile tests were carried out according to ASTM E21 standard [28] using cylindrical specimens machined in rolling direction with a reduced section diameter of 6 mm and a gauge length of 30 mm. The tensile tests were performed in the temperature range of 300-800°C under two various strain rates of 2×10^{-4} and 2×10^{-3} s^{-1} using an Instron-4208 universal testing machine. This was followed by quenching specimens in water just after straining. The small elastic deflection of the machine and grips were ignored. The temperature control was within ±2°C. The obtained data was calculated and represented as true stress-true strain and elongation-to-fracture vs. temperature curves. The true stress-strain curves are plotted considering the constant volume rule ($A_0L_0 = AL$), and the curves over the necking contain errors coming from volume change due to cavitation. The flow stress in engineering curves essentially declines after the necking which is described considering the geometrical aspect of uniaxial tensile test. However, in spite of the engineering curve, the true

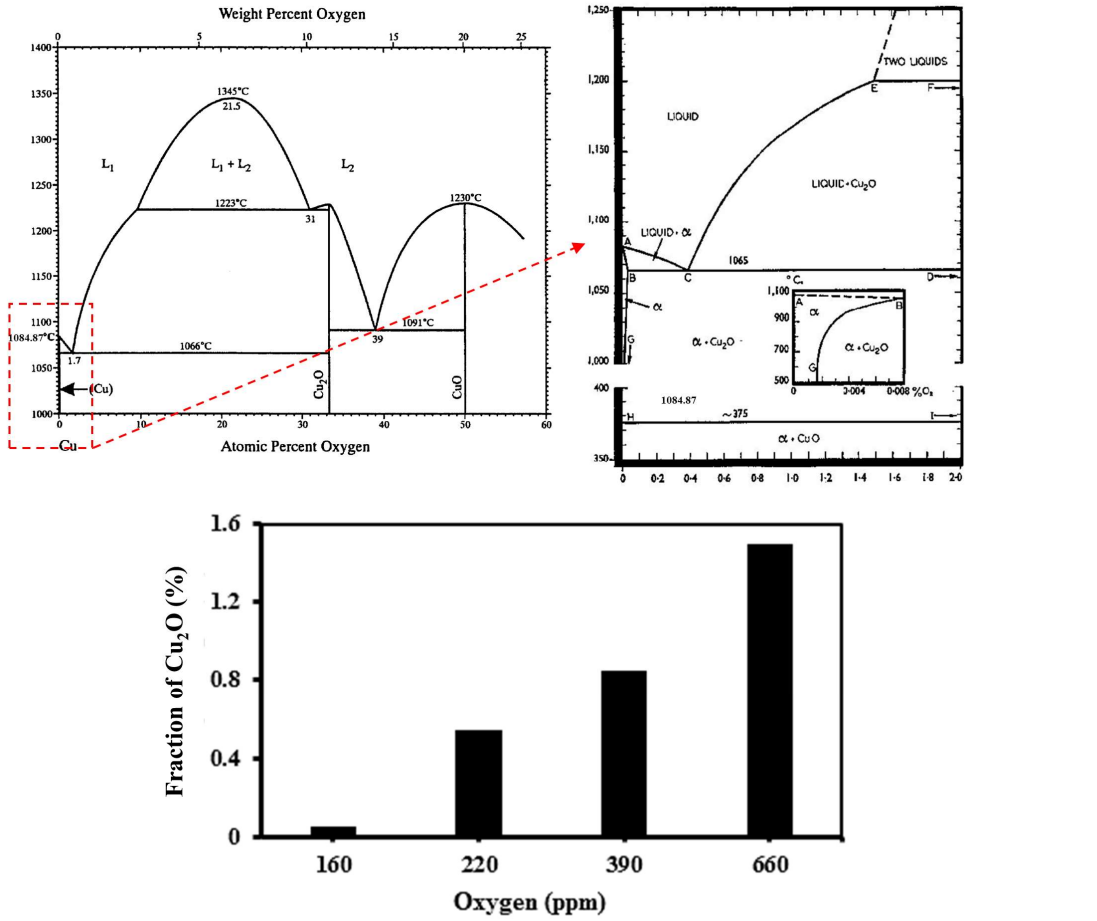

Fig. 1. Copper-oxygen equilibrium phase diagram representing the solid soluability of oxygen at variuous temperatures [27]. The density of Cu_2O vs. oxygen content calculated according to Cu_2O equilibrium phase diagram.

one is expected to follow a continuous hardening trend up to the fracture, so the observed softening region can be considered as a clue to roughly judge the activation of restoration mechanisms and susceptibility to crack growth. In addition, related fracture surfaces were also examined using a scanning electron microscope (SEM) to explain the corresponding hot ductility behavior of the alloys.

In order to properly clarify dominant restoration processes, inter alia, dynamic recrystallization and dynamic recovery, the hot compression test was also conducted at the same temperatures and strain rates. Cylindrical compression specimens were machined holding the size of 8 mm in diameter and 12 mm in height in accordance with the ASTM E209 standard [29]. Prior to any hot compression or tensile test, the specimens were first preheated to the preset temperature and soaked for 7 min to equilibrate the temperature throughout the specimens. After compressive straining up to the predetermined strain of 0.5, the compressed specimens were cut, cold mounted, polished, and etched by 50 ml NH_4OH dissolving in the 50 ml H_2O_2 etchant. Optical microscopy was performed to characterize the microstructural changes of deformed specimens at specified thermomechanical conditions.

3. Results and Discussion

3.1. The hot compression behavior

3.1.1. Temperature and strain rate effect

The initial microstructure of the starting material is depicted in Fig. 2a. Due to the previous heavily cold rolling program (high reduction of area and short time annealing at relatively low temperature), the trace of parent elongated grains can be characterized through the microstructure. However, it can also be deduced that the annealing heat treatment could relatively turn the grains morphology into the equiaxed configuration. In order to examine the general changing trend of the grain size by increasing the deformation temperature, the initial specimens have been annealed at 400, 600, and 800°C for 1 h and their microstructures have been compared (Fig. 2b-2c). The corresponding mean grain sizes are measured to be 20, 50, and 250 µm, respectively. As is

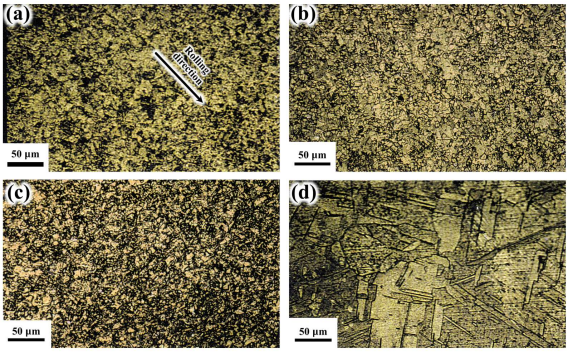

Fig. 2. The optical microstructures of the (a) starting material and the annealed specimens at (b) 400°C, (c) 600°C, and (d) 800°C.

expected, the obtained results reveal the growing initial grain size by increasing the temperature especially over the transition range of 0.3-0.5 T_m. Moreover, the appearance of annealing twins at higher temperatures, along with the copper oxide second phases, is truly noticeable. The effect of grain size on high temperature deformation behavior of the experimented alloy will be discussed in the next sections.

The compressive true stress-true strain curves of the specimens containing 390 ppm oxygen content at the temperature range of 300-600°C under the initial strain rate of 2×10^{-3} s^{-1}, are represented in Fig. 3. As is shown, the overall characteristics of the flow curves are significantly affected by the deformation temperature as follows. All curves exhibit a broad peak stress, followed by dynamic softening regime that suggests the occurrence of typical dynamic recrystallization which is more possible in the case of metals in which recovery processes are slow, such as those holding low or medium stacking fault energy (copper, nickel, and austenitic

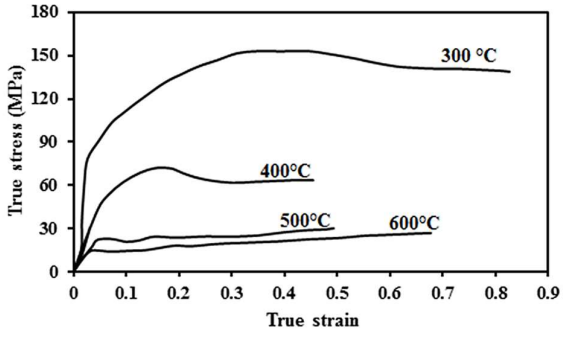

Fig. 3. Compressive true stress-strain curves of copper containing 390 ppm oxygen under the strain rate of 2×10^{-3} s^{-1}.

iron). The corresponding compressive deformed microstructures are given in Fig. 4. In comparison to the starting microstructure, the existence of fine equiaxed grains is considered as proper evidence for the occurrence of dynamic recrystallization.

Additionally, in order to assess the strain rate effect on the compressive flow behavior, the obtained results under the lower strain rate of 2×10^{-4} s^{-1} are also included in Fig. 5. The flow characteristics well verify the capability of the experimented copper for dynamic recrystallization in the specified high temperature deformation regime. It is worth to note that some of the stress-strain curves of this dynamically recrystallizing material are characterized by a single peak and others by several oscillations (multiple peaks). In other words, the resultant curves at lower temperatures of 300 and 400°C contain a single dynamic recrystallization peak, whereas, by increasing the temperature up to 600°C, the multiple peaks are revealed. Such evidence can be uniquely discussed relying on the variation of the Zener-Hollomon parameter (Z). The Zener-Hollomon parameter is a parameter in the field of thermomechanical processing through which the effects of temperature and strain rate on the deformation behaviors can be characterized simultaneously [23-26] and are described as follows:

$$Z = \dot{\varepsilon} \exp(\frac{Q}{RT}) \quad (1)$$

At high Zener-Hollomon (Z) parameter (lower temperatures and higher strain rates), subsequent cycles of recrystallization begin before the previous one ends, the material is therefore always in a partly recrystallized state after the first peak, and the stress-strain curve is smoothed out, resulting in a single broad peak. Moreover, by increasing the Z value, the peak stress and critical strain of recrystallization (σ_p and ε_c) increased (Fig. 6). In other words, at low temperatures and high strain rates (high Z) the dislocation generation (work

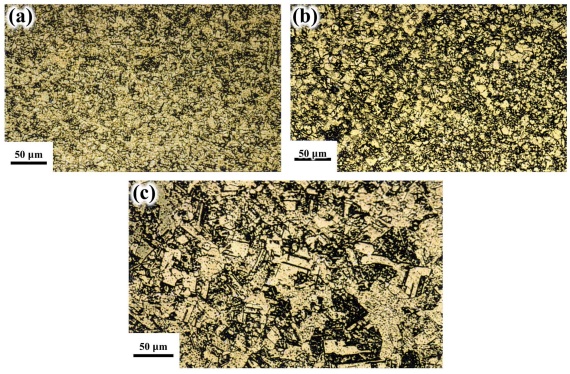

Fig. 4. Microstructures of copper containing 390 ppm oxygen which have been compressed at (a) 300, (b) 400, and (c) 500°C under the strain rate of 2×10^{-3} s^{-1}.

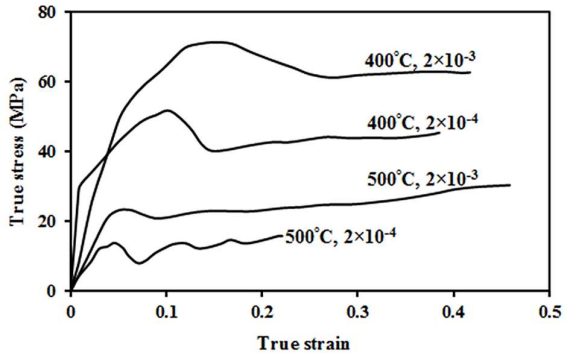

Fig. 5. Compressive true stress-strain curves of copper containing 390 ppm oxygen at 400°C and 500°C under different strain rates.

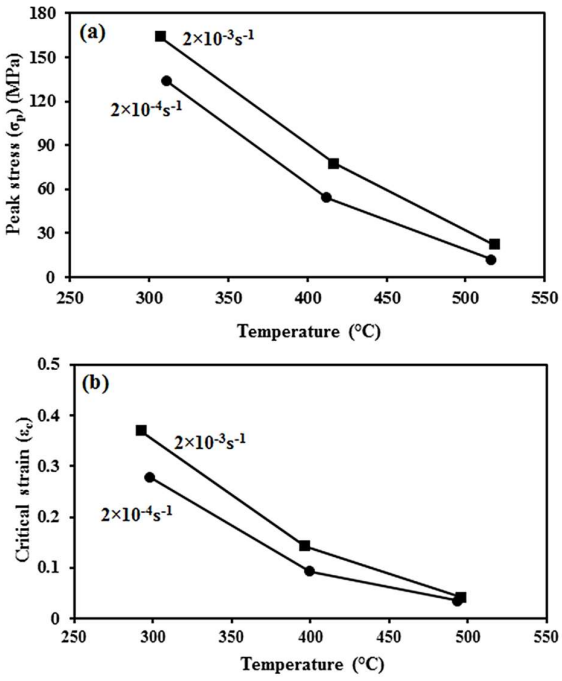

Fig. 6. The variation of (a) peak stress and (b) critical strain of dynamic recrystallization by temperature. The presented results have been extracted from the compressive true stress-strain curves of copper containing 390 ppm oxygen at 400°C and 500°C under different strain rates.

hardening) factor is dominant and recrystallization process is retarded. In contrast, under the conditions of low Z value (higher temperatures and lower strain rates), the material recrystallizes completely before the second cycle of recrystallization begins, and this process is then repeated, and multiple peaks are exhibited at low strains. Correspondingly, by decreasing the Z parameter, σ_p and ε_c decreased. This phenomenon has been previously discussed by other researchers in the case of various metals and alloys [30, 31]. As is evident, the flow stress characteristics of pure copper are significantly dependent on the temperature and the strain rate.

3.1.2. Oxygen content effect

The compressive true stress-true strain curves of the experimental alloy holding 160, 220 and 390 ppm oxygen contents at 500 and 600°C under the strain rate of 2×10^{-4} s^{-1} are depicted in Fig. 7. As is observed, the multiple peaks dynamic recrystallization has been activated in the case of all microstructures having different oxygen contents. In a more detailed view, the variation of peak stress and critical strain vs. oxygen content are given in Fig. 8. As can be seen, the peak stress (σ_p) and critical strain (ε_c) of dynamic recrystallization decrease by increasing the oxygen content up to 220 ppm. However, corresponding values increase with further oxygen content increment of up to 390 ppm (and also up to 660 ppm). This is in accordance with the previously reported results by Ravichandran and Prasad et al. [32]. The presence of oxygen as interstitial atoms which act like barriers against dislocation movement through solute dragging effect, increases the rate of dislocation tangling and capability of subsequent rearrangement at an appropriate deformation temperature. This apparently results in increasing the rate of dynamic recrystallization nucleation through the possible continuous or discontinuous mechanisms, and hence, lowering the amount of critical strain. This well justify the observed trend to up to 220 ppm content. The maximum solid solubility of the oxygen is about 50 ppm at 900°C, the rest of which will be present in the form of the Cu_2O particles, especially at higher concentrations. At the higher oxygen content (above 220 ppm) the fraction of oxide particles increases, and the fine oxides may pin the

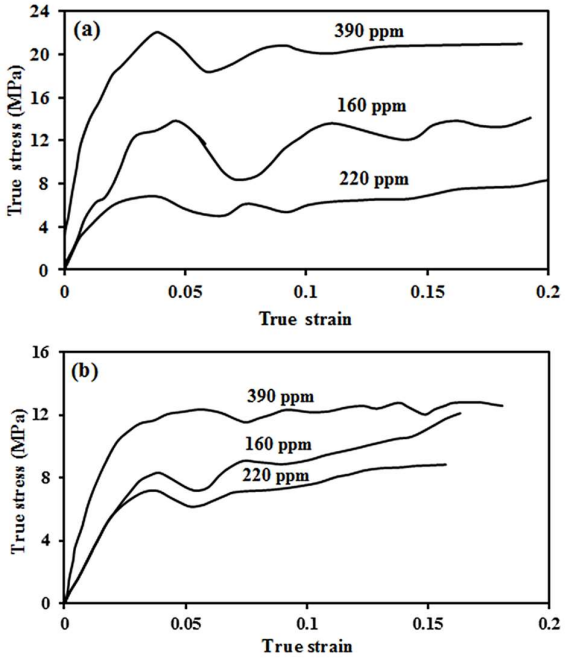

Fig. 7. The effect of oxygen content on compressive true stress-true strain curves conducted under the strain rate of 2×10^{-4} s^{-1} at (a) 500°C and (b) 600°C.

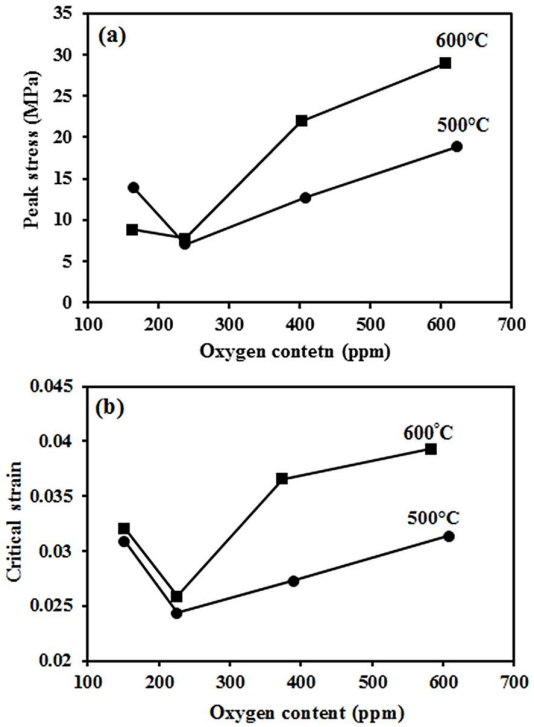

Fig. 8. The effect of oxygen content (ppm) on the critical strain and critical stress values obtained through hot compression test.

grain boundaries and resist against grain boundary migration (boundary bulging) as the main micro-mechanism of discontinuous recrystallization. This is known as the main responsible factor for the retardation of dynamic recrystallization at higher oxygen content that finally increases the critical strain.

It should be noted that the coarse oxide particles may also impose a large back stress against dislocation movement and increase the possibility of dynamic recrystallization through particles stimulated nucleation (PSN) mechanism. However, the contribution of such continuous mechanism is not considerable in pure copper with relatively low stacking fault energy (~41mJ/mm^2), and the discontinuous recrystallization is generally considered as a dominant mechanism. As a result, the effect of oxygen, both as interstitials and oxides on the dynamic recrystallization depending on the operating mechanism, needs to be more clearly stated and will be the subject of our future studies.

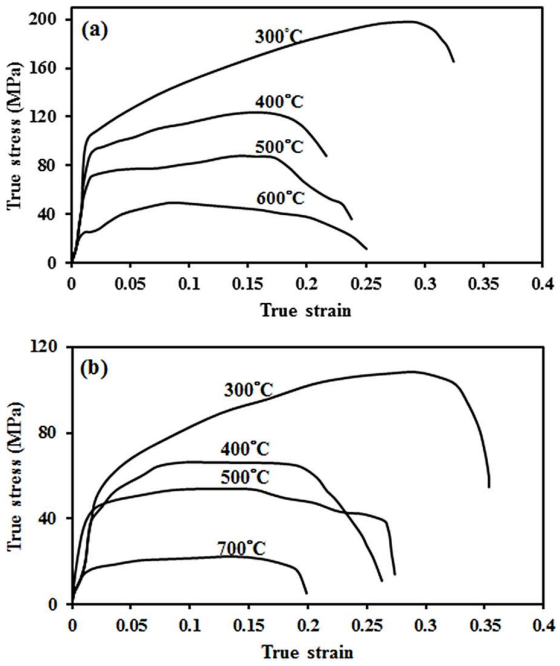

Fig. 9. Tensile true stress-strain curves of the copper containing (a) 160 and (b) 390 ppm oxygen. The tests have been conducted under the strain rate of 2×10^{-4} s^{-1}.

3.2. The tensile test results

3.2.1. Influence of the temperature and oxygen content

The typical true stress-strain curves of the specimens holding different oxygen contents, 160 and 390 ppm, which have been deformed in tensile mode at different temperatures are shown in Fig. 9. The copper containing 160 ppm oxygen indicate a maximum strength of about 200 MPa with a maximum elongation to fracture nearby 0.35 at 300°C. In the corresponding flow curve, the imposed strain is mainly accommodated through uniform elongation and accompanied by a high work hardening rate. This is followed by a short post-UTS region. Increasing the deformation temperature results in decreasing the strength levels, the work hardening rate and the portion of the pre-UTS region (the uniform elongation). However, the non-uniform elongation region increased by increasing the temperature. Above 500°C this region was the dominant portion of curves. Generally, the flow softening in the tensile curve is invariably associated with geometric instability related to the necking, which generally gives rise to a short post-UTS region [9]. The long post-uniform elongation and the correlated low work hardening rate obtained at temperatures higher than 500°C is well attributed to the occurrence of dynamic recrystallization. The occurrence of the restoration phenomena increases the resistance of the material to localized necking and provides a proper condition for diffused/sustained necking [10, 11]; and this properly justifies the obtained high non-uniform elongation values. In the case of copper with 390 ppm oxygen content, the same results have been obtained although the flow stress levels have shifted to lower values. Insignificant differences in elongation to fracture values in both copper at the same thermomechanical conditions may be attributed to their relatively high capability for the occurrence of dynamic recrystallization as was observed in corresponding compressive flow curves. Despite our previous findings in compression mode, the specimen holding higher oxygen content of 390 ppm possess lower flow stress level. This well emphasize the fact that the effectiveness of oxide particles as a dislocation barrier is completely different under the tensile and compressive mode of deformation. It seems that the previously defined threshold for oxygen content (220 ppm) has been shifted

to higher values under the tensile mode of deformation. The oxygen as interstitials or oxides plays the same role in compression or tensile mode of deformation, and the observed variation can be well justified considering the different dislocation maneuverability under the different modes of deformation.

3.2.2. Hot ductility behavior

The variation of elongation to fracture values vs. deformation temperature at a specified strain rate have been plotted for the specimens holding various oxygen contents (Fig. 10). All curves indicate similar ductility rises and falls and two ductility drop regions at 400±50°C (region I) and 600±50°C (region II), respectively. As a matter of fact, the oxygen content does not have any sensible effect on the position of minimum ductility temperatures. On the other hand, the variation of elongation-to-fracture as a function of test temperature at different strain rates is presented in Fig. 11. The obtained curves designate that the ductility trough of region I shifts to the lower temperature of 300±50°C when increasing the strain rate from 2×10^{-4} s^{-1} to 2×10^{-3} s^{-1}. Details of ductility variation at different deformation conditions have been described point by point and are as follows.

3.2.2.1. Ductility drop in region I

For fractography analyses, the specimen holding 390 ppm oxygen content has been selected as representative microstructure. The detailed investigation of fracture surfaces of the specimens which have been deformed at 300 and 400°C under different strain rates (Fig. 12) exhibited ductile mode of fracture. Ductile dimples with different sizes and depth without any cleavage facet can be clearly observed on fracture surfaces. At such relatively low temperature regime, the ductile dimples have mainly originated from second phase particles dispersed through the microstructure especially on the grain boundaries. As is seen, the remarkable morphology changes on fracture surfaces through the variation of temperature and strain rate are attributed to the number, size and depth of ductile dimples. The shallow dimples are mainly observed on the fracture surface of the specimens which have been deformed under the lower strain rate. It seems that the materials possess higher capability to tolerate the progress of cavitation process under the higher strain rate. This is in agreement with the positive effect of increasing strain rate on the material's ductility (Fig. 11).

Considering the impossibility of grain boundary sliding (GBS) under the specified thermomechanical

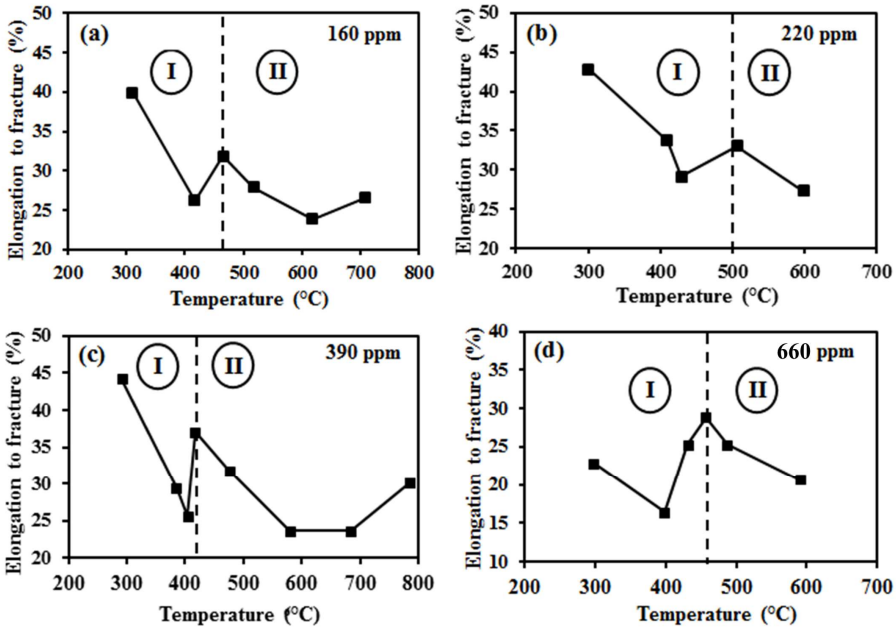

Fig. 10. Elongation to fracture vs. temperature curves under the 2×10^{-4} s^{-1} strain rate for the specimens containing (a) 160 ppm; (b) 220 ppm; (c) 390 ppm; (d) 660 ppm Oxygen.

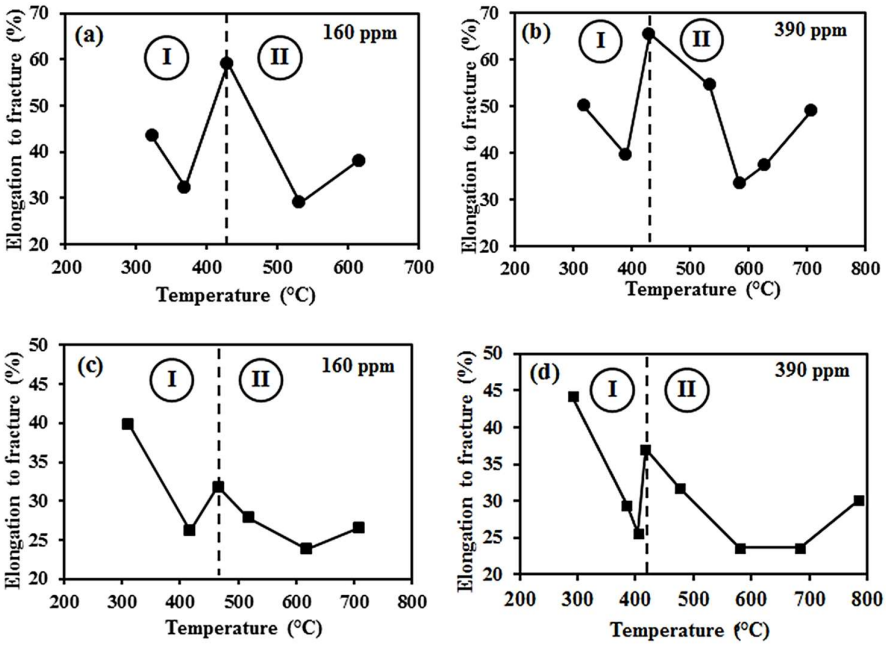

Fig. 11. Elongation to fracture-temperature curves for the specimens with two different oxygen contents which have been deformed under the strain rates of (a) and (b) 2×10^{-3} s^{-1}; (c) and (d) 2×10^{-4} s^{-1}.

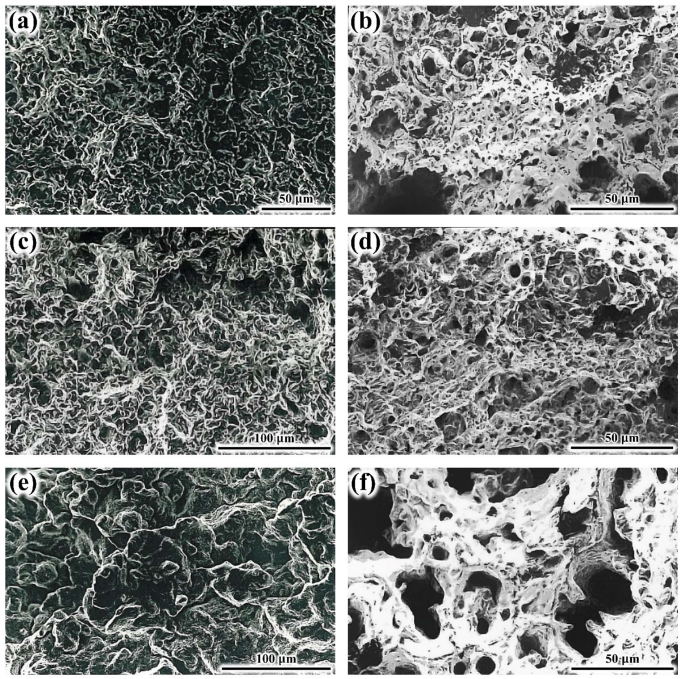

Fig. 12. The fracture surface of tensile deformed specimens under the strain rate of 2×10^{-4} s^{-1} at: (a) T=400°C, (c) T=300°C, (e) T=600°C, and under the strain rate of $2\times10^{-3}s^{-1}$ at: (b) T=400°C, (d) T=300°C and (f) T=600°C. The fracture surfaces belong to the specimen holding 390ppm oxygen content as representative microstructure.

conditions, the observed ductility drop can be discussed by relying on the presence of second phase particles (Cu_2O) and the possible formation of precipitation-free zones (PFZs) at the vicinity of grain boundaries. It has been shown that the formation of the PFZs, due to their different elastic modulus and plastic deformation behavior with parent matrix, increases the strain incompatibility and the probability of shear flow

localization. This means a higher rate of cavity nucleation and growth, which results in increasing the length of micro-cracks [33]. However, by increasing the temperature above 400°C, the mobility of high angle grain boundaries increases and, as a result, dynamic recrystallization activates through strain induced boundary migration. As a consequence, the cavities and discontinuities, which are being formed in the microstructure, are isolated from the grain boundaries as a preferred path of crack growth. Therefore, the growth and the coalescence of these cavities have not readily taken place and the strain to fracture beyond the necking increases.

3.2.2.2. Ductility drop in region II

The fracture surfaces of the specimens which have been deformed at 600°C under various strain rates are shown in Fig. 13. All fracture surfaces obtained under 2×10^{-5} s^{-1} demonstrate a dendritic fracture mode that alters into the dimple fracture mode by increasing the strain rate to 2×10^{-2} s^{-1}. This is further approved considering the variation of elongation to fracture vs. strain rate at 600°C for the specimen holding 390 ppm oxygen content (Fig. 14). In a more detailed view, the tensile flow curves of annealed specimens at 300, 400, 600, and 800°C by the average grain sizes of 5, 20, 50, and 250 µm which have been tested at 600°C /2×10^{-4} s^{-1} are given in Fig. 15. As can be seen, by increasing the initial grain size up to 250 µm, the strength and ductility values increase as well. The corresponding fracture surface characteristics (Fig. 16) also verify the higher formability of the microstructure holding higher grain size. The effect of strain rate and grain size on the material's ductility well indicate the contribution of GBS as the dominant deformation mechanism. In fact, the stress concentration triggered at pinned grain boundaries by Cu_2O particles during boundary sliding may cause the development of W-type or R-type cracks thereby reducing the ductility. Increasing the grain size and imposed strain rate, decreases the possibility of cracking and results in higher formability. In contrast, the boundary sliding may have a great contribution to the total deformation if well accommodated through other

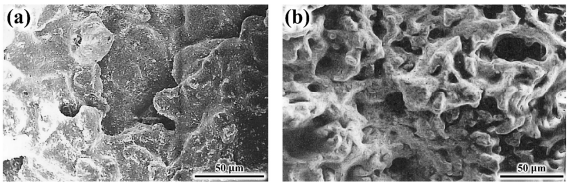

Fig. 13. The fracture surfaces of the specimens (holding 390 ppm oxygen content) which have been deformed at 600°C under the strain rate of (a) 2×10^{-5} s^{-1}, and (b) 2×10^{-2} s^{-1}.

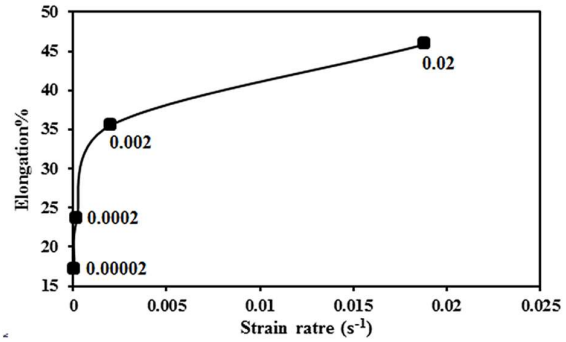

Fig. 14. The variation of elongation to fracture vs. the strain rate at 600°C for the specimen containing 390 ppm oxygen.

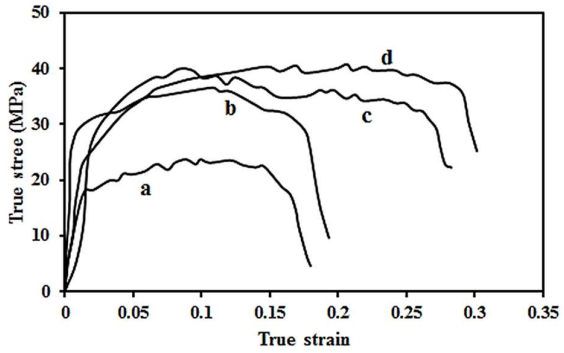

Fig. 15. True stress-strain curves of annealed specimens holding different grain sizes of (a) 5, (b) 20, (c) 50, and (d) 250 µm which have been deformed at 600°C /2×10^{-4} s^{-1}.

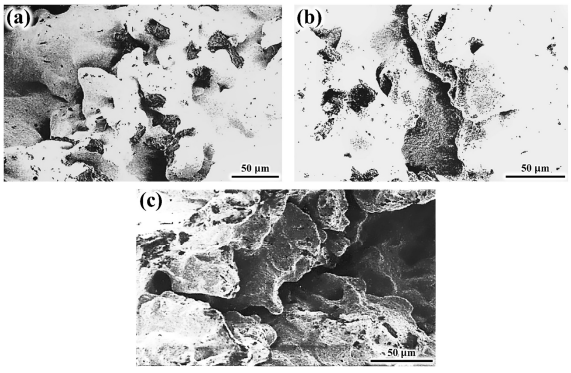

Fig. 16. The fracture surface of tensile specimens deformed at 600°C under the strain rate of 2×10^{-4} s^{-1} holding the initial grain size of (a) 20 µm, (b) 50 µm, and (c) 250 µm. These fracture surfaces belong to the microstructures which have been annealed at 400, 600, and 800°C, respectively (Fig. 3).

mechanisms such as diffusional flow and dislocation slip. In this respect, by further increasing the deformation temperature, the effect of the second phase particles' pinning decreases, thereby inducing higher mobility of grain boundaries during GBS. Consequently, the effect of second phase particles on the cavity nucleation and growth would reduce and the enhanced ductility regime can be successfully attained.

Finally, it should be noted that the main advantage of the present work is conducting a comprehensive mechanical testing to investigate the effect of (1) deformation temperature, (2) strain rate and strain, (3) grain size, (4) deformation mode (compression or tension), and (5) oxygen content on the hot ductility behavior of tough pitch copper. The observations have been also discussed in correlation with the fracture surface characteristics of the deformed materials. However, the main lack of the present work is the establishment of microstructure-properties relationship which seems to be more complex and requires in-detail TEM and EBSD studies (for instance to elucidate the precipitation free zone or particle stimulated nucleation). In this respect, the local investigation of the microstructure is not adequate and surveying through the starting and deformed microstructures, which is the subject of our future work, is essential.

4. Conclusion

The ductility behavior of tough pitch copper containing different contents of oxygen was studied by conducting tensile tests in a wide range of temperatures (300-800°C). The hot compression tests were also executed at the same temperature range to characterize activated restoration processes. The following conclusions have been drawn:

1. At high Zener-Hollomon parameter, the deformed microstructure was always in a partly recrystallized state. The subsequent cycles of recrystallization started before the previous ones had finished, and resulted in appurtenance of single broad peak in compressive flow curves. In contrast, at higher temperatures and lower strain rates (low Z value), the microstructures recrystallized completely before the second cycle of recrystallization began, and this process was then repeated and multiple peaks were observed at low strains.
2. Dynamic recrystallization was motivated by increasing the oxygen content up to 220 ppm. However, the required critical strain decreased once more with further oxygen content increment up to 390 ppm. This acceleration/deceleration was discussed considering the effect of oxygen in the solute state on the dislocation tangling and subsequent substructure development, or in oxide form on the grain boundary pinning.
3. A ductility drop was recognized at 400±50°C (region I). The ductility trough shifted to the lower temperatures after increasing the strain rate. The oxygen content, however, did not have any tangible effects on the position of minimum ductility temperatures.
4. The moderate ductility improvement above 450°C was attributed to the activation of dynamic recrystallization process. The development of dynamically recrystallized grains through grain boundary migration isolated the micro-cracks away from the preferred growth path and improved ductility values.
5. By increasing the temperature up to 600°C, a ductility trough associated with the activation of grain boundary sliding, also appeared at 600±50°C (region II). The stress concentration resulted from pinning the grain boundaries by Cu_2O particles caused development of W-type or R-type cracks thereby reducing the elongation to fracture values. Ductility improvement at higher temperatures (above 650°C) was attributed to the increased mobility of the grain boundaries.

Conflict of Interests

The authors declare that they have no known competing financial interests or personal relationships that could have appeared to influence the work reported in this paper.

Funding

This research received no specific grant from any funding agency in the public, commercial, or not-for-profit sectors.

5. References

[1] B. Mintz, S. Yue, J.J. Jonas, Hot ductility of steels and its relationship to the problem of transverse cracking during continuous casting, *International Materials Reviews*, 36(1) (1991) 187-220.

[2] B. Mintz, The influence of composition on the hot ductility of steels and to the problem of transverse cracking, *ISIJ international*, 39(9) (1999) 833-855.

[3] I. Mejíaa, A. Bedolla-Jacuinde, C. Maldonado, J.M. Cabrera, Hot ductility behavior of a low carbon advanced high strength steel (AHSS) microalloyed with boron, *Materials Science and Engineering: A*, 528(13-14) (2011) 4468-4474.

[4] A. Haft Baradaran, A. Zarei-Hanzaki, H. Abedi, S. Fatemi-Varzaneh, A. Imandoust, The ductility behavior of a high-Mn twinning induced plasticity steel during cold-to-hot deformation, *Materials Science and Engineering: A*, 561 (2013) 411-418.

[5] A.S. Hamada, L.P. Karjalainen, Hot ductility behaviour of high-Mn TWIP steels, *Materials Science and Engineering: A*, 528(3) (2011), 1819-1827.

[6] R. Nowosielski, P. Sakiewicz, P. Gramatyka, The effect of ductility minimum temperature in CuNi25 alloy, *Journal of Materials Processing Technology*, 162 (2005) 379-384.

[7] W. Ozgowicz, The relationship between hot ductility and intergranular fracture in a CuSn6P alloy at elevated temperatures, *Journal of Materials Processing Technology*, 162 (2005) 392-401.

[8] M.H. Ghavam, M. Morakabati, S.M. Abbasi, H. Badri, Hot ductility behavior of near-alpha titanium alloy IMI834, *International Journal of Materials Research*, 105(11) (2014) 1090-1096.

[9] H.R. Abedi, A. Zarei-Hanzaki, S. Khoddam, Effect of γ precipitates on the cavitation behavior of wrought AZ31 magnesium alloy, *Materials & Design*, 32(4) (2011) 2181-2190.

[10] O. Sabokpa, A. Zarei-Hanzaki, H.R. Abedi, Mater, An investigation into the hot ductility behavior of AZ81 magnesium alloy, *Materials Science and Engineering: A*, 550 (2012) 31-38.

[11] M. Taheri-Mandarjani, A. Zarei-Hanzaki, H.R. Abedi, Hot ductility behavior of an extruded 7075 aluminum alloy. *Materials Science and Engineering: A*, 637 (2015) 107-122.

[12] W.L. Chan, M.W. Fu, J. Lu, J.G. Liu, Modeling of grain size effect on micro deformation behavior in micro-forming of pure copper, *Materials Science and Engineering: A*, 527(24-25) (2010) 6638-6648.

[13] W.L. Chan, M.W. Fu, B. Yang, Study of size effect in micro-extrusion process of pure copper, *Materials & Design*, 32(7) (2011) 3772-3782.

[14] B. Yang, C. Motz, M. Rester, G. Dehm, Yield stress influenced by the ratio of wire diameter to grain size–a competition between the effects of specimen microstructure and dimension in micro-sized polycrystalline copper wires, *Philosophical Magazine*, 92(25-27) (2012) 3243-3256.

[15] A.T. Jennings, M.J. Burek, J.R. Greer, Microstructure versus size: mechanical properties of electroplated single crystalline Cu nanopillars, Physical Review Letters, 104(13) (2010) 135503.

[16] J.Q. Su, T.W. Nelson, T.R. Mc Nelley, R.S. Mishra, Development of nano-crystalline structure in Cu during friction stir processing (FSP), *Materials Science and Engineering: A*, 528(16-17) (2011) 5458-5464.

[17] T. Sakai, H. Miura, X. Yang, Ultrafine grain formation in face centered cubic metals during severe plastic deformation, *Materials Science and Engineering: A*, 499(1-2) (2009) 2-6.

[18] K. Youssef, M. Sakaliyska, H. Bahmanpour, R. Scattergood, C. Koch, Effect of stacking fault energy on mechanical behavior of bulk nanocrystalline Cu and Cu alloys, *Acta Materialia*, 59(14) (2011) 5758-5764.

[19] X.Y. San, X.G. Liang, L.P. Chen, Z.L. Xia, X.K. Zhu, Influence of stacking fault energy on the mechanical properties in cold-rolling Cu and Cu–Ge alloys, *Materials Science and Engineering: A*, 528(27) (2011) 7867-7870.

[20] A. Belyakov, T. Sakai, H. Miura, K. Tsuzaki, Grain refinement in copper under large strain deformation, *Philosophical Magazine A*, 81(11) (2001) 2629-2643

[21] H. Khodaverdizadeh, A. Mahmoudi, A. Heidarzadeh, E. Nazari, Effect of friction stir welding (FSW) parameters on strain hardening behavior of pure copper joints, *Materials & Design*, 35 (2012) 330-334.

[22] F. Cao, I.J. Beyerlein, F.L. Addessio, B.H. Sencer, C.P. Trujillo, E.K. Cerreta, G.T. Gray III, Orientation dependence of shock-induced twinning and substructures in a copper bicrystal, *Acta Materialia*, 58(2) (2010) 549-559.

[23] H. Zhang, H.G. Zhang, D.S. Peng, Hot deformation behavior of KFC copper alloy during compression at elevated temperatures, *Transactions of Nonferrous Metals Society of China*, 16(3) (2006) 562-566.

[24] S.H. Huang, D.Y. Shu, C.K. Hu, S.F. Zhu, Effect of strain rate and deformation temperature on strain hardening and softening behavior of pure copper, *Transactions of Nonferrous Metals Society of China*, 26(4) (2016) 1044-1054.

[25] S. H. Huang, S.X. Chai, X.S. Xia, Q. Chen, D.Y. Shu, Compression deformation behaviour and processing map pf pure copper, *Strength of Materials*, 48 (2016) 98-106.

[26] A. Belyakov, H. Miura, T. Sakai, Dynamic recrystallization under warm deformation of polycrystalline copper, *ISIJ International*, 38(6) (1998) 595-601.

[27] M. Heinemann, B. Eifert, C. Heiliger, Band structure and phase stability of the copper oxides Cu_2O, CuO, and Cu_4O_3, *Physical Review B*, 87(11) (2013) 115111.

[28] ASTM E21, Standard test methods for elevated temperature tension tests of metallic materials, ASTM International, 1988.

[29] ASTM E209, Standard practice for compression tests of metallic materials at elevated tmperatures with conventional or rapid heating rates and strain rates, ASTM International, 2010.

[30] F.J. Humphreys, M. Hatherly, Recrystallization and related annealing phenomena, Elsevier, 2004.

[31] P. Zhao, T.S.E. Low, Y. Wang, S.R. Niezgoda, An integrated full-field model of co-current plastic deformation and microstructure evolution: Application to 3D simulation of dynamic recrystallization in polycrystalline copper, *International Journal of Plasticity*, 80 (2016) 38-55.

[32] N. Ravichandran, Y.V.R.K. Prasad, Influence of oxygen on dynamic recrystallization during hot working of polycrystalline copper, *Materials Science and Engineering: A*, 156(2) (1992) 195-204.

[33] B.H. Chen, H. Yu, Hot ductility behavior of V-N and V-Nb microalloyed steels, *International Journal of Minerals, Metallurgy, and Materials*, 19(6) (2012) 525-529.